Identification of new alpha-synuclein fibrillogenesis inhibitor using in silico structure-based virtual screening

Mehdi Sahihi [a,b,*], Fatma Gaci [b], Isabelle Navizet [b]

[a] Roberval Laboratory, Université de Technologie de Compiègne, Alliance Sorbonne Université, Compiègne, France
[b] MSME, Univ Gustave Eiffel, CNRS UMR 8208, Univ Paris Est Creteil, F-77454, Marne-la-Vallée, France

ARTICLE INFO

ABSTRACT

Abnormal aggregation and accumulation of alpha-synuclein (αSN) in existing neurons is associated with Parkinson's disease (PD) as one of the age-related neurodegenerative disorders. Inhibition of αSN fibrillogenesis could be considered as a solution for PD diseases treatment. Here, virtual screening (VS) approach was used to investigate available ligands in PubChem library with structural similarity with Dihydromyricetin (DHM) (as a recently introduced suitable candidate for designing of novel antiPD drugs) against aggregation of αSN chains. Primary screening identified 314 promising molecules for αSN monomer, which were further analyzed in details by their binding energy and binding modes through molecular docking method. Evidently, the compound with PubChem ID of 100968625 displayed the lowest free binding energy with $\Delta G^0 = -7.1$ kcal.mol^{-1} and was selected for further analysis using molecular dynamics (MD) simulation method. Analysis of MD trajectories showed that molecules of the selected ligand interact with αSN trimer via H-bond interaction and destabilize the compact structure of αSN trimer. Further, prompt *in vivo* testing to validate the antiPD inhibition efficiency by this molecule can save lives.

1. Introduction

One of the age-related neurodegenerative disorders is Parkinson's disease (PD) of which the frequency increases with the increase in age. About 2–3% of people over 65 years old worldwide suffer from the disease [1]. This disease characterized by occurrence of Lewy bodies (LBs) which is formed by abnormal aggregation and accumulation of alpha-synuclein (αSN) in existing neurons [2,3]. αSN is a 140 amino acids protein (molecular weight of about 14 kDa) with significant conformational flexibility that can adopt a wide range of structural conformations such as fibrils and oligomers [4,5]. The native structure of αSN is not still exactly defined and has been described as intrinsically disordered protein (IDP) [6,7], helical [8,9], or a mixture of both [10]. While the function of αSN is unclear, it is highly enriched in neurons, where it is present in the presynaptic cleft as well as mitochondrial membranes. As for Alzheimer's disease (AD), for which certain oligomers of the amyloidogenic protein are toxic, the initiation of formation of αSN aggregate is suspected to be a key step in PD disease formation [11]. The cytotoxic effect of these aggregates could be because of their effect on lipid membrane permeabilisation, mitochondrial damage and oxidative stress [12]. Also, recent experimental studies have shown that the injection of αSN aggregates in animal's brain can stimulate their prion-like spread in other brain regions [13]. Most of the available drugs for PD are chemicals acting as a prodrug that will be converted in dopamine in the brain [14,15] or are dopamine agonists inhibiting the enzymes responsible of dopamine metabolism [16,17]. Both of these sorts of medicines cause unwanted side effects such as headaches, nausea, somnolence and so on [17]. Hence, inhibition of αSN fibrillogenesis and disaggregation of αSN fibrils by therapeutic medications could provide a more significant neuroprotective effect against PD diseases [18,19]. Nowadays, finding of compounds that can work as robust inhibitors of αSN fibrillogenesis remains an important challenge. Given the enormous set of existing compounds, it is impossible to perform experimental screening of all available databases in a reasonable timeframe. Advances in computational chemistry provide new opportunities to steer experiments with realistic simulations on how the available compounds may be manipulated to introduce new effective inhibitor for αSN aggregation at minimum cost.

Virtual screening (VS) is known as one of the effective methods to recognize novel bioactive compounds and is being used in many drug discovery and development strategies at the moment. In this method, the chemical entities of big libraries are rapidly screened to achieve

---

structures with better ligand-receptor interaction pattern. In most of the VS strategies docking methods are applied on the large databases [20, 21].

Flavonoids are one of the large class of natural compounds that are mainly found in plant-derived materials and display antioxidant [22,23] and anti-carcinogenic activities [24–26]. The ability of flavonoids to bind to carrier proteins [27–29] as well as their effects against cancer [30] and nicotine-induced oxidative stress [31] have been validated by a large number of investigations. Dihydromyricetin (DHM; Fig. S1) is a flavonoid compound isolated from *Ampelopsis grossedentata* (a traditional southern Chinese herb), that has several physiological and pharmacological effects [32]. Especially, DHM showed neuroprotective against oxidative stress and valuable effects in neurodegenerative diseases [33]. Recently, Jia et al. found that DHM could inhibit αSN fibrillogenesis and destabilize mature αSN fibrils in a dose-dependent manner [34]. Their findings suggested that DHM has a great potential to be developed into a new aggregation inhibitor for αSN. Since DHM inhibits αSN fibrillogenesis and destabilizes mature αSN fibrils, its derivatives would be suitable candidates for designing of novel antiPD drugs with inhibitory effects on aggregation of αSN.

Therefore, in the present work the following computational studies have been done to design new αSN aggregation inhibitor using VS strategy:

1 More than 8600 compounds with similar chemical structure to DHM were chosen from PubChem free database [35].
2 These compounds have been filtered on basis of Lipinski's "Rule of five" and topological polar surface area (TPSA)
3 The binding properties of the 314 remained compounds with αSN monomer have been investigated using molecular docking tools.
4 By considering the results of the VS part, the compound with lowest binding energy was chosen to perform a 100 ns molecular dynamics (MD) simulation of its complex with a αSN trimer to investigate its effect as potential inhibitor for αSN aggregation.

2. Computational procedures

2.1. Building a library of the drug-like compounds

Structure based VS is one of the common techniques being used in primary phases of drug design, discovery and development at pharmaceutical companies and academic groups [36]. To build a library of candidate molecules, the structure of DHM was selected as template and similar structures were saved from PubChem free database. The physicochemical characteristics of small molecular drugs have an important effect on their Blood-Brain barrier (BBB) permeability. Based on Lipinski's rule of five, a small molecular drug must have less than 5 H-bond donors, less than 10 H-bond acceptors, be smaller than 500 Da of molecular weight, and its calculated octanol-water partition coefficient (log *P)* should be less than 5 to have an appropriate BBB permeability [37]. The log *P* value of a compound is the logarithm of its partition coefficient between n-octanol and water (log ($c_{octanol}/c_{water}$)) and is an extent of the compound's hydrophilicity. The ideal range for BBB permeability has been found to be 1.5–2.5 [38]. We used the Lipinski's rule of five from the filters available in the PubChem database to select the candidate molecules for the VS. Then, the topological polar surface area (TPSA; as a commonly used medicinal chemistry metric for the optimization of a drug's ability to permeate cells) was calculated using Molinspiration webserver (www.molinspiration.com). Therefore, only compounds with TPSA between 20 and 130 Å^2 were kept in the VS database [39]. DHM and 314 other ligands met the criteria.

2.2. Molecular docking

The experimental structure of αSN saved from PDB (PDB ID: 1XQ8) database [40]. This structure has been obtained by average structure

criteria using solution NMR method. The water molecules of the.pdb file were removed and hydrogen atoms, charges, standard bond orders and the missing residues were added using Build/Check/Repair model wizard in WHAT IF web interface [41]. Minimization was carried out up to 500 steps by steepest descent method using GROMACS 2018 package [42] with GROMOS96 53A6 force field [43]. The structures of the obtained drug-like compounds were saved in.sdf format and converted to. pdbqt format using PyRx 0.8 software as input files for VS [44]. The chemical structure of DHM and the 314 other ligands (obtained after filtration by Lipinski's rule of five and TPSA calculations) were geometry optimized by AM1 semi empirical level of theory using Gaussian 09 quantum chemistry package [45] and are represented in Table S1. The blind molecular docking of DHM to αSN monomer was carried out using AutoDock Vina [46] which is an academic-free molecular docking (and virtual screening) software and works based on empirical scoring functions. The molecular docking was done based on a semi-flexible docking mechanism with a rigid receptor and flexible ligand. The default parameters were assigned for molecular docking calculations and the pose with the lowest binding energy was chosen as final result. For the other compounds obtained from PubChem database, the center of the docking box was set in the center of the DHM binding site and the same procedure was done.

2.3. MD simulation

The initial structure of αSN trimer used in the MD simulation has been obtained from its available amyloid fibril structure determined by cryo-electron microscopy (PDB ID: 6A6B [47]). All MD simulations were performed using the GROMACS 2018 package [42] with GROMOS96 53A6 force field [43]. The force field parameters of the selected ligand (the small molecule with the most negative binding energy to αSN monomer) were obtained from prodrg web server [48] and Lemkul's method [49] was used to correct the atomic partial charges. The αSN trimer was put in a cubic box with periodic boundary conditions (PBC) in three directions. The protein trimer was placed in the center of the box and the minimum distance between solute surface and the box was set to 1.0 nm. Ten molecules of the selected ligand were randomly placed around the αSN trimer. Then, the box was filled with SPC water molecules [50] and the system was neutralized by replacing six water molecules with Chloride ions (Cl⁻). In parallel, a system of αSN trimer without the ligand molecules was also prepared. The systems were energy minimized using 50000 steps of the steepest descent method and were equilibrated for 1 ns in NVT followed by 1 ns in NPT ensembles. Finally, a 100 ns MD simulation was carried out at 1 bar and 300 K for each system. Berendsen thermostat [51] Parrinello–Rahman barostat [52,53] and 1 nm cutoff for van der Waals (vdW) and Coulomb interactions were applied. Also, the long-range electrostatics were considered by particle mesh Ewald (PME) method [54,55] and the equations of motion were integrated by leap-frog algorithm with a time step of 2 fs. Finally, the atomic coordinates were recorded to the trajectory file every 0.5 ps for later analysis.

3. Results and discussion

3.1. Virtual screening and molecular docking

Considering the structural similarity with DHM as a representative inhibitor for αSN aggregation, 8609 compounds were obtained from PubChem database. The obtained compounds were filtered using Lipinski's rule of five considering their Hydrogen bonding capacity, molecular weight, and calculated log *P* as well as good TPSA. Finally, 314 out of 8609 compounds were selected as potential satisfied drug with possibility of good absorption or permeability through the BBB.

The previously published experimental results suggest that IDPs remain disordered in their bound state [56]. Hence, the αSN monomer was chosen to investigate its affinity for DHM binding. A molecular
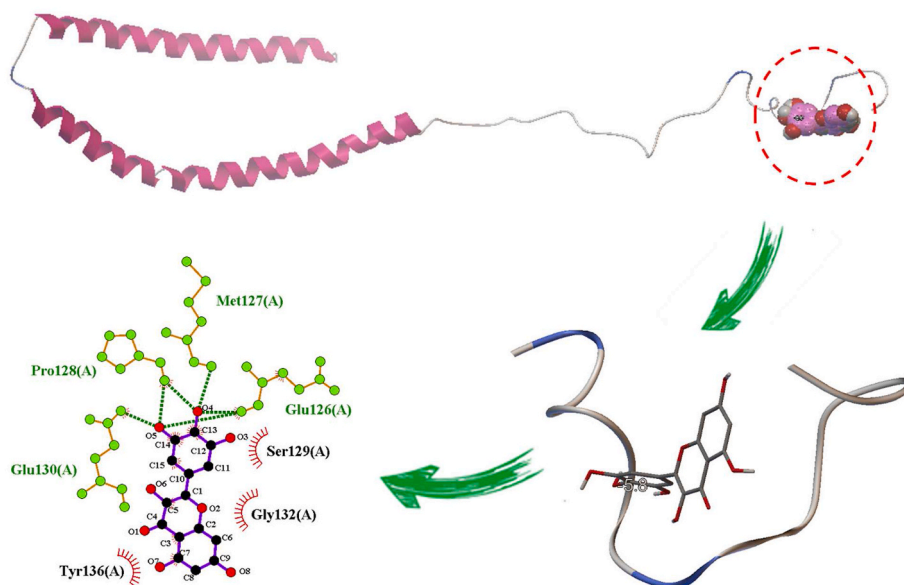
Fig. 1. Docking pose of αSN-DHM complex. H-bond and hydrophobic interactions are represented as green dashed lines and red curves, respectively. (For interpretation of the references to colour in this figure legend, the reader is referred to the Web version of this article.)
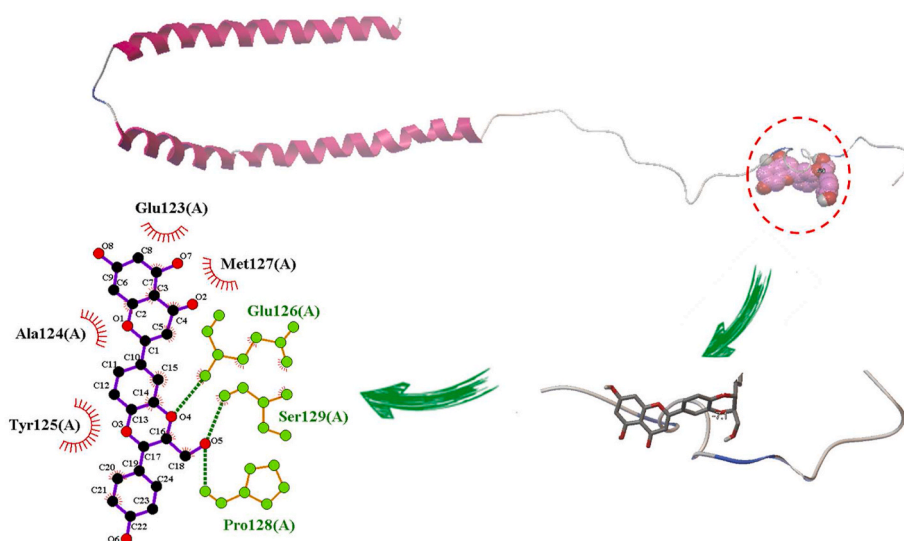
Fig. 2. Docking pose of the most stable complex of the selected ligand and αSN monomer. H-bond and hydrophobic interactions are represented as green dashed lines and red curves, respectively. (For interpretation of the references to colour in this figure legend, the reader is referred to the Web version of this article.)

docking study was carried out to find out the preferred location and conformation of DHM on αSN monomer. The docking pose of the most stable DHM-αSN complex is represented in Fig. 1. The results reveal that DHM binds to the terminal part of αSN monomer's IDP domain which is the αSN binding site for rosmarinic acid [57]. The standard binding free energy (ΔG^0) of this interaction is about -5.8 kcal.mol^{-1}. The molecular complex system shows six H-bond interactions between DHM and Glu126, Met127, Pro128 and Glu130 residues of αSN. These H-bond interactions accompanied by hydrophobic interactions may have key roles in the stability of the system.

Then, 314 compounds that passed the Lipinski's rule of five and TPSA filtering were subjected to molecular docking (Table S1). These molecules were docked to the DHM binding site of αSN monomer. Achieved docked poses for each compound were ranked by their binding energies and conformations with the most negative binding energy were selected as main binding pose. Results revealed that 61 compounds among them showed lower binding energies than DHM. These

compounds were highlighted in Table S1. The compound with PubChem ID 100968625 (IUPAC name: 5,7-dihydroxy-2-[(2R,3R)-3-(hydroxymethyl)-2-(4-hydroxyphenyl)-2,3-dihydro-1,4-benzodioxin-6-yl]chromen-4-one, Fig. S2) displayed the lowest binding free energy ($\Delta G^0 = -7.1$ kcal.mol^{-1}) and was selected for further analysis. The value of calculated binding free energy is very close to the obtained values for polyphenols of *Ocimum sanctum* (OS) extract which its inhibitory effect on αSN aggregation has been studied, before [57].

Moreover, the calculated log *P* value of this molecule is about 2.4 that makes it as a good BBB permeable drug. Fig. 2 represents the docking pose of the most stable complex of the selected ligand and αSN monomer. Analysis of the docking results reveals that there are three H-bond interactions between the ligand and Glu126, Pro128 and Ser129 residues of αSN. All binding energies and key residues involved in the interactions of DHM, candidate molecule and the other first 21 screened compounds with the highest binding energies, with αSN monomer are summarized in Table 1. These results revealed that H-bond, hydrophobic

Table 1
Binding energies and key residues involved in the interactions of DHM (and the first 22 screened compounds with the highest binding energies) and αSN monomer.

Rank	Name or PubChem ID	Binding Energy/ kcal. mol^{-1}	H-bond interactions	Hydrophobic interactions	π-π interactions
–	DHM	−5.8	Glu126, Met127, Pro128, Glu130	Gly 132, Tyr 136	–
1	100968625	−7.1	Glu126, Pro128, Ser129	Glu 123, Ala 124, Tyr 125, Met 127	–
2	6280229	−7.0	Glu 126	Tyr 125, Met 127, Ser 129, Glu 130, Gly 132, Ala 140	Tyr 136
3	129825792	−6.9	Glu 126	Ser 129, Gly 132, Ala 140	Tyr 125, Tyr 136
4	129905005	−6.8	Glu 126, Met 127	Ser 129, Glu 130, Gly 132, Tyr 136	Tyr 125
5	5315126	−6.7	Glu 126, Pro 128	Tyr 125, Glu 130, Glu 131, Gly 132, Tyr 136	–
5	5467201	−6.7	Glu 126	Met 127	Tyr 125, Tyr 136
5	71313853	−6.7	–	Glu 126, Pro 128, Glu 130	Tyr 125
5	90643991	−6.7	Pro 128	Glu 126, Glu 130, Glu 131, Gly 132, Tyr 136	–
6	14427462	−6.5	Glu 126, Tyr 136	Tyr 125, Glu 126, Met 127, Pro 128, Glu 130, Gly 132	Tyr 136
6	67984060	−6.5	–	Glu 123, Glu 126, Pro 128, Ser 129	–
6	90643985	−6.5	Met 127	Glu 126, Ser 129, Glu 130, Gly 132, Tyr 136	Tyr 125
6	90643986	−6.5	–	Glu 126, Gly 132, Tyr 136	Tyr 125
6	90643987	−6.5	Glu 126	Tyr 125, Ser 129, Gly 132, Tyr 136	–
6	129825797	−6.5	Glu 126	Ser 129, Glu 130, Gly 132, Tyr 136	–
6	129904975	−6.5	Met 127	Glu 126, Ser 129, Glu 130, Gly 132, Tyr 136	Tyr 125
7	5315125	−6.4	Glu 126	Tyr 125, Glu 130, Gly 132, Tyr 136	–
7	14427460	−6.4	Pro 128	Tyr 125, Met 127, Glu 130, Glu 131, Gly 132	Tyr 136
7	23630406	−6.4	–	Glu 126, Ser 129, Glu 130, Glu 131, Tyr 136	–
8	580166	−6.3	–	Glu 126, Ser 129, Glu 131	Tyr 125
8	13349170	−6.3	–	Tyr 125	–
8	13834128	−6.3	Met 127	Tyr 125, Glu 126, Pro 128, Glu 131	–

Table 1 (*continued*)

Rank	Name or PubChem ID	Binding Energy/ kcal. mol^{-1}	H-bond interactions	Hydrophobic interactions	π-π interactions
8	18542127	−6.3	–	Tyr 125, Glu 126, Glu 130, Gly 132, Asp 135	–

and π-π interactions have dominant roles in binding of candidate molecules to αSN monomer.

3.2. MD simulation
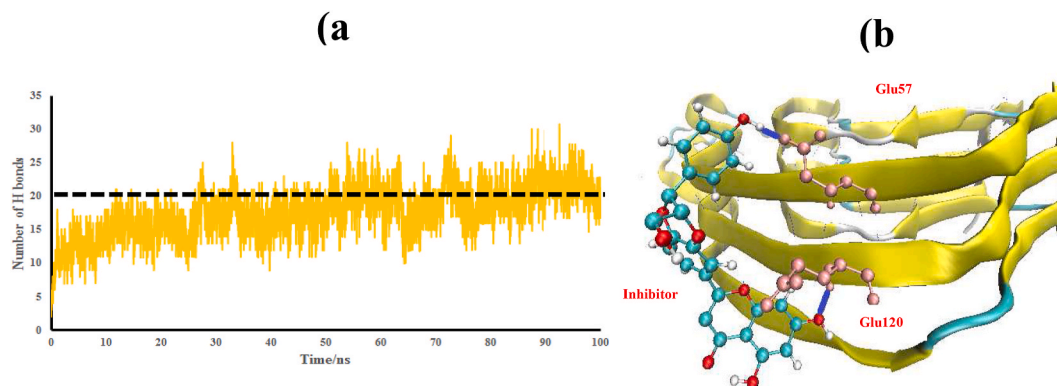
The interactions between ten molecules of the selected ligand (PubChem ID: 100968625) and a αSN trimer was investigated using MD simulations method. The selected ligand (Fig. S2) contains a carbonyl group, two ether oxygen atoms, and five hydroxyl groups that can interact with αSN via H-bond interaction. This makes a total of 8 possible H-bond sites for each ligand molecule. Therefore, the total number of H-bonds formed between the αSN trimer and the ten ligand molecules was calculated and shown in Fig. 3. Analysis of the results showed that H-bonds were formed between the αSN trimer and ligands, rapidly after few ns of MD simulation trajectory and their number increased to about 20 at around 30 ns and fluctuated around this mean value until the end (about 2 H-bonds per ligand molecule). Fig. 3b shows the representative structure of αSN and one of the ligands molecules interacting by H-bond interactions. It shows that there was a H-bond interaction between hydrogen atom of the hydroxyl group of the ligand and an oxygen atom of the carboxyl group of the side chain of the residue Glu57. Same interaction has been reported for the interaction of DHM molecules with αSN trimer [34]. At the same time, there was another hydrogen bond between the same ligand and the amide group of residue.

This observation is completely in agreement with the docking results and proves the key role of H-bond interactions in the stability of inhibitor-αSN complex. Furthermore, the previously published results have confirmed that H-bond interactions have important role in the interaction of their suggested inhibitors and αSN protein [21,34,57,58]. The compactness of αSN trimer during the MD simulations (in the presence and absence of the selected compound) is an important factor to study the inhibitory effect of the candidate drug and conformational changes of the protein trimer during its interaction with it. Therefore, the radius of gyration (R_g) of the αSN trimer was evaluated as an index of protein structural compactness. Fig. 4 shows that the R_g of αSN trimer in the presence of the selected compound increased in comparison to the case without the compound indicating the less compact structure of αSN trimer (Fig. 4). The average values of R_g are about 2.03 and 2.11 nm for free αSN and its complex with 10 molecules of the candidate drug, respectively. This observation proves that the compound destabilizes the compact structure of αSN trimer.

To evaluate the mobility of the residues of αSN trimer, the root mean square fluctuations (RMSF) of the residues of protein aggregate in the absence and presence of inhibitor were analyzed and presented in Fig. 5.

The results of the RMSF analysis indicate that all the residues of αSN trimer show higher fluctuations in the presence of inhibitor molecules in comparison to the state without inhibitors. This observation is in consistency with the R_g results and could be another evidence about good inhibitory effect of the selected compound as new inhibitor of αSN aggregation. The middle chain (chain II in Fig. 5) of the αSN trimer has been surrounded between two other chains and is not accessible for the inhibitor molecules as much as two other chains. This protection causes its less fluctuations in comparison to the chains I and III of the protein trimer in both states (in the presence and absence of the inhibitors).

Fig. 3. Interaction of the selected ligand (PubChem ID: 100968625) with the αSN timer. (a) Total number of hydrogen bonds between the αSN trimer and the ten ligand molecules during 100 ns of MD simulation. (b) Binding conformation between residues in the αSN trimer and one of the ligand molecules at the end of trajectory. The blue solid lines represent the H-bonds. Glu residues have been shown as pink ball & stick representation. (For interpretation of the references to colour in this figure legend, the reader is referred to the Web version of this article.)
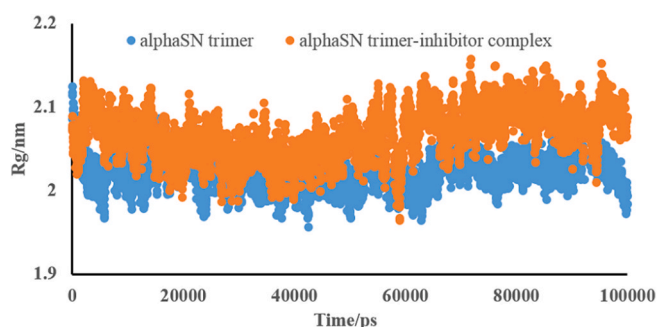
Fig. 4. Time dependence of the radius of gyration (R_g) for αSN trimer during the simulation, in the absence and presence of inhibitor.
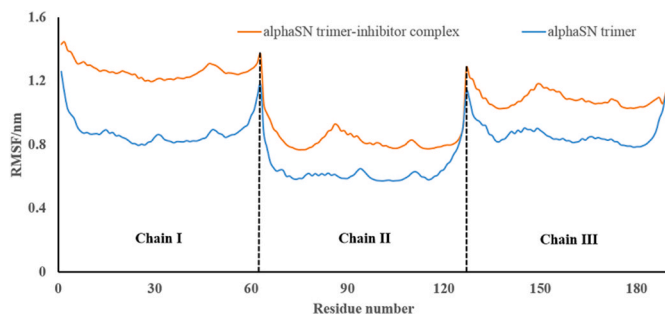
Fig. 5. RMSF values of residues of αSN trimer during the 100 ns of simulation time, in the absence and presence of the inhibitor. (Chain I: residues 1-63; Chain II: residues 64-126 and Chain III: residues 127-189).

Fig. 6 represents that during 100 ns of MD simulation trajectory, most of the inhibitor molecules associate in N-terminal of the protein trimer that causes higher fluctuation of this part in three chains of αSN trimer as it is clear in Fig. 5. In the presence of the inhibitor, the N-terminal fluctuations of the three chains are about 14%, 15% and 18% higher than C-terminal for Chains I to III, respectively. However, the maximum RMSF difference between the N- and C-terminal in the absence of the inhibitor would be only about 7% (for chain I). In other words, the interaction of inhibitor molecules with αSN chains weakens the intermolecular interactions between the N-terminal residues of the protein trimer and increase the fluctuations of the residues in this part of the protein. Furthermore, one inhibitor molecule inserts into the interspace between two chains of the αSN trimer, which would disturb the intermolecular interactions between the chains. To prove this claim, the

distance between the Cα atoms of Glu57 of chain I and Glu120 of chain II was calculated as shown in Fig. 7. The average distance in the presence of inhibitor was about 12 Å after 20 ns, while the distance in the αSN trimer in water was nearly 5 Å during the entire simulation time. Therefore, insertion of the inhibitor molecule inside the inner space of the αSN chains caused a loss of contact between two chains and disrupted their initial ordered structure.

4. Conclusion

In this study, we built a library of compounds with similar structure of Dihydromyricetin (DHM; a natural flavonoid with inhibitory effect on αSN fibrillogenesis). Lipinski's "Rule of five" and TPSA screenings were used to select the drug like compounds. Moreover, binding free energy and binding modes of the filtered compounds were investigated using in silico virtual screening method. The analysis of the molecular docking calculations showed that the compound with PubChem ID of 100968625 has the highest affinity for binding to αSN monomer ($\Delta G^0_{binding} = -7.1$ kcal.mol^{-1}) among the other candidates. Its high binding affinity for αSN suggested that this compound could be considered as an inhibitor for αSN aggregation with higher efficiency than DHM and some of the other previously suggested antiPD drugs. The behavior of αSN trimer in the presence of the selected candidate was further analyzed using molecular dynamics (MD) simulation method. Analysis of MD trajectories showed that H-bond interactions between the hydroxyl groups of the ligand molecules with side chains of the residues in αSN trimer could destabilize the compact structure of αSN trimer. On the other hand, most of the inhibitor molecules associate in N-terminal of the protein trimer and cause 100% increasing of fluctuations for the residues in N-terminal of the trimer structure. Also, investigation of R_g of the αSN trimer showed that the inhibitor molecules decrease the compactness of protein structure for about 4% in comparison to the protein free state in water. Furthermore, penetration of one inhibitor molecule into the interspace of two protein chains, disturbed the ordered structure of the αSN filament, weakened the intermolecular interactions between the protein chains and increased their distance. In conclusion, our study revealed the inhibitory effect of selected ligand (PubChem ID = 100968625) on αSN fibrillogenesis. Eventually, we believe that this study will shed the lights on finding of potentially active compounds against the αSN aggregation. We also confirm that it is necessary to do further in vitro and *in vivo* investigations for developing potent drug inhibitors of αSN fibrillogenesis for the treatment of PD and similar diseases.

Declaration of competing interest

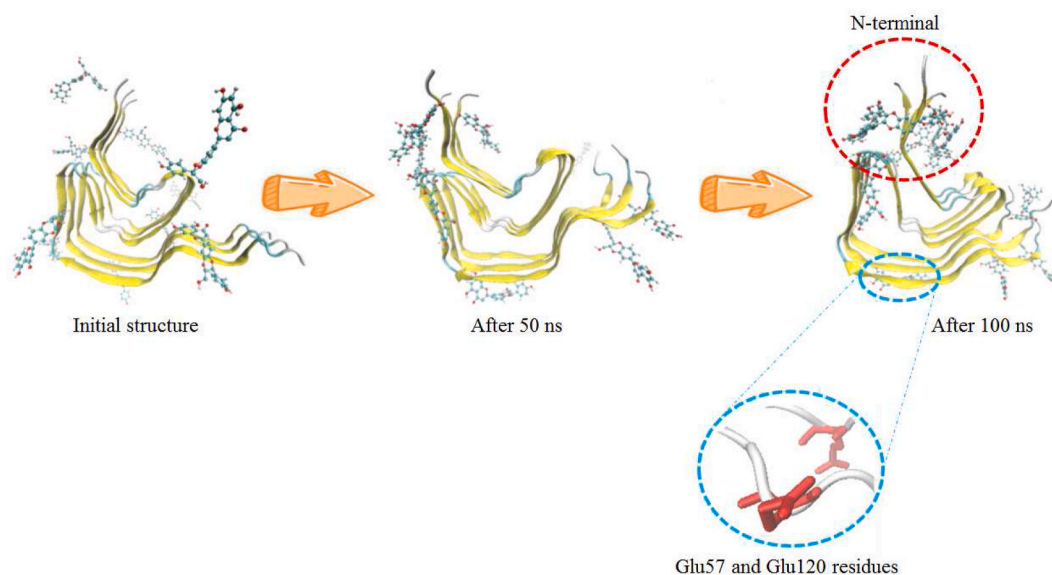The authors declare that they have no known competing financial

Fig. 6. Configuration of the ligand molecules around αSN trimer during 100 ns of MD simulation.

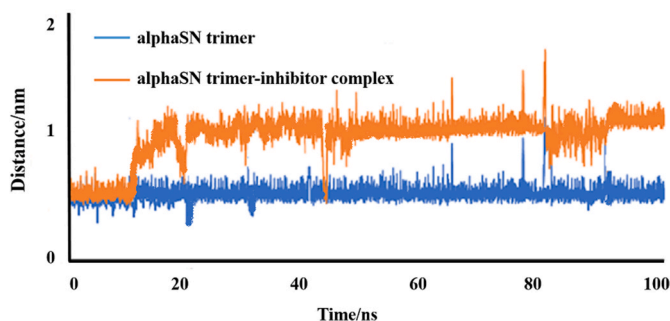**Fig. 7.** Change of Glu57-Glu120 distance in chains I and II of αSN trimer during the simulation, in the absence and presence of inhibitor.

interests or personal relationships that could have appeared to influence the work reported in this paper.

Acknowledgments

Appendix A. Supplementary data

Supplementary data to this article can be found online at https://doi.org/10.1016/j.jmgm.2021.108010.

References

[1] W. Poewe, et al., Parkinson disease, Nat. Rev. Dis. Prim. 3 (1) (2017) 1–21, https://doi.org/10.1038/nrdp.2017.13.
[2] F.H. Lewy, *Paralysis agitans. I.* Pathologische Anatomie, Handbuch der neurologie, 1912.
[3] L. Xu, J. Pu, Alpha-synuclein in Parkinson's disease: from pathogenetic dysfunction to potential clinical application, Parkinson's Dis. 2016 (2016), https://doi.org/10.1155/2016/1720621.
[4] A. Deleersnijder, et al., The remarkable conformational plasticity of alpha-synuclein: blessing or curse? Trends Mol. Med. 19 (6) (2013) 368–377, https://doi.org/10.1016/j.molmed.2013.04.002.
[5] S. Mehra, S. Sahay, S.K. Maji, α-Synuclein misfolding and aggregation: implications in Parkinson's disease pathogenesis, Biochim. Biophys. Acta Protein Proteomics 1867 (10) (2019) 890–908, https://doi.org/10.1016/j.bbapap.2019.03.001.
[6] L. Breydo, J.W. Wu, V.N. Uversky, α-Synuclein misfolding and Parkinson's disease, Biochim. Biophys. Acta (BBA) - Mol. Basis Dis. 1822 (2) (2012) 261–285, https://doi.org/10.1016/j.bbadis.2011.10.002.
[7] F.-X. Theillet, et al., Structural disorder of monomeric α-synuclein persists in mammalian cells, Nature 530 (7588) (2016) 45–50, https://doi.org/10.1038/nature16531.
[8] T. Bartels, J.G. Choi, D.J. Selkoe, α-Synuclein occurs physiologically as a helically folded tetramer that resists aggregation, Nature 477 (7362) (2011) 107–110, https://doi.org/10.1038/nature10324.
[9] W. Wang, et al., A soluble α-synuclein construct forms a dynamic tetramer, Proc. Natl. Acad. Sci. Unit. States Am. 108 (43) (2011) 17797–17802, https://doi.org/10.1073/pnas.1113260108.
[10] J. Burré, et al., Properties of native brain α-synuclein, Nature 498 (7453) (2013) E4–E6, https://doi.org/10.1038/nature12125.
[11] B. Winner, et al., In vivo demonstration that α-synuclein oligomers are toxic, Proc. Natl. Acad. Sci. Unit. States Am. 108 (10) (2011) 4194–4199, https://doi.org/10.1073/pnas.1100976108.
[12] L. Ma, et al., Non-polyphenolic natural inhibitors of amyloid aggregation, Eur. J. Med. Chem. 192 (2020), 112197, https://doi.org/10.1016/j.ejmech.2020.112197.
[13] S. Sangwan, et al., Inhibition of synucleinopathic seeding by rationally designed inhibitors, Elife 9 (2020), e46775, https://doi.org/10.7554/eLife.46775.
[14] A. Chakraborty, S. Brauer, A. Diwan, A review of possible therapies for Parkinson's disease, J. Clin. Neurosci. 76 (2020) 1–4.
[15] F. Haddad, et al., Dopamine and levodopa prodrugs for the treatment of Parkinson's disease, Molecules 23 (1) (2018) 40.
[16] T.B. Stoker, K.M. Torsney, R.A. Barker, Front. Neurosci. 12 (2018) 693, https://doi.org/10.3389/fnins.2018.00693.
[17] I. Carrera, R. Cacabelos, Current drugs and potential future neuroprotective compounds for Parkinson's disease, Curr. Neuropharmacol. 17 (3) (2019) 295–306.
[18] O.M. El-Agnaf, et al., A strategy for designing inhibitors of α-synuclein aggregation and toxicity as a novel treatment for Parkinson's disease and related disorders, Faseb. J. 18 (11) (2004) 1315–1317, https://doi.org/10.1096/fj.03-1346fje.
[19] Y. Nagai, et al., Inhibition of polyglutamine protein aggregation and cell death by novel peptides identified by phage display screening, J. Biol. Chem. 275 (14) (2000) 10437–10442, https://doi.org/10.1074/jbc.275.14.10437.
[20] S. Vittorio, et al., Rational design of small molecules able to inhibit α-synuclein amyloid aggregation for the treatment of Parkinson's disease, J. Enzym. Inhib. Med. Chem. 35 (1) (2020) 1727–1735, https://doi.org/10.1080/14756366.2020.1816999.
[21] S.S. Jafaripour, et al., In silico drug repositioning of FDA-approved drugs to predict new inhibitors for alpha-synuclein aggregation, Comput. Biol. Chem. 88 (2020), 107308.
[22] F.A. van Acker, et al., Flavonoids can replace α-tocopherol as an antioxidant, FEBS Lett. 473 (2) (2000) 145–148, https://doi.org/10.1016/S0014-5793(00)01517-9.
[23] J. Yu, et al., Antioxidant activity of citrus limonoids, flavonoids, and coumarins, J. Agric. Food Chem. 53 (6) (2005) 2009–2014, https://doi.org/10.1021/jf0484632.
[24] S. Kawaii, et al., Quantitation of flavonoid constituents in citrus fruits, J. Agric. Food Chem. 47 (9) (1999) 3565–3571, https://doi.org/10.1021/jf990153+.
[25] D. Pszczola, Natural Colors: Pigments of Imagination, Food technology, USA), 1998.
[26] H.C. Cooray, et al., Biochem. Biophys. Res. Commun. 317 (1) (2004) 269–275, https://doi.org/10.1016/j.bbrc.2004.03.040.

[27] I. Khosravi, M. Sahihi, Computational studies on the interaction of arctiin and liquiritin with β-lactoglobulin, J. Macromol. Sci., Part B 53 (9) (2014) 1591–1600, https://doi.org/10.1080/00222348.2014.946844.

[28] M. Sahihi, In-silico study on the interaction of saffron ligands and beta-lactoglobulin by molecular dynamics and molecular docking approach, J. Macromol. Sci., Part B 55 (1) (2016) 73–84, https://doi.org/10.1080/00222348.2015.1125066.

[29] M. Sahihi, Y. Ghayeb, Binding of biguanides to β-lactoglobulin: molecular-docking and molecular dynamics simulation studies, Chem. Pap. 68 (11) (2014) 1601–1607, https://doi.org/10.2478/s11696-014-0598-7.

[30] R.J. Williams, J.P. Spencer, C. Rice-Evans, Flavonoids: antioxidants or signalling molecules? Free Radical Biol. Med. 36 (7) (2004) 838–849, https://doi.org/10.1016/j.freeradbiomed.2004.01.001.

[31] B. Sengupta, et al., Differential roles of 3-Hydroxyflavone and 7-Hydroxyflavone against nicotine-induced oxidative stress in rat renal proximal tubule cells, PloS One 12 (6) (2017), e0179777, https://doi.org/10.1371/journal.pone.0179777.

[32] T. Murakami, et al., Hepatoprotective activity of tocha, the stems and leaves of Ampelopsis grossedentata, and ampelopsin, Biofactors 21 (1–4) (2004) 175–178.

[33] X. Kou, et al., Ampelopsin attenuates 6-OHDA-induced neurotoxicity by regulating GSK-3β/NRF2/ARE signalling, J. Funct. Foods 19 (2015) 765–774, https://doi.org/10.1016/j.jff.2015.10.010.

[34] L. Jia, et al., Dihydromyricetin inhibits α-synuclein aggregation, disrupts preformed fibrils, and protects neuronal cells in culture against amyloid-induced cytotoxicity, J. Agric. Food Chem. 67 (14) (2019) 3946–3955, https://doi.org/10.1021/acs.jafc.9b00922.

[35] S. Kim, et al., PubChem 2019 update: improved access to chemical data, Nucleic Acids Res. 47 (D1) (2019) D1102–D1109, https://doi.org/10.1093/nar/gky1033.

[36] S.B. Mirza, et al., Discovery of selective dengue virus inhibitors using combination of molecular fingerprint-based virtual screening protocols, structure-based pharmacophore model development, molecular dynamics simulations and in vitro studies, J. Mol. Graph. Model. 79 (2018) 88–102, https://doi.org/10.1016/j.jmgm.2017.10.010.

[37] C.A. Lipinski, et al., Experimental and computational approaches to estimate solubility and permeability in drug discovery and development settings, Adv. Drug Deliv. Rev. 23 (1–3) (1997) 3–25, https://doi.org/10.1016/S0169-409X(96)00423-1.

[38] J.L. Mikitsh, A.-M. Chacko, Pathways for small molecule delivery to the central nervous system across the blood-brain barrier, Perspect. Med. Chem. 6 (2014), S13384, https://doi.org/10.4137/pmc.s13384. PMC.

[39] Z. Jin, et al., Structure-based virtual screening of influenza virus RNA polymerase inhibitors from natural compounds: molecular dynamics simulation and MM-GBSA calculation, Comput. Biol. Chem. 85 (2020), 107241.

[40] T.S. Ulmer, et al., Structure and dynamics of micelle-bound human α-synuclein, J. Biol. Chem. 280 (10) (2005) 9595–9603, https://doi.org/10.1074/jbc.M411805200.

[41] G. Vriend, What IF: a molecular modeling and drug design program, J. Mol. Graph. 8 (1) (1990) 52–56, https://doi.org/10.1016/0263-7855(90)80070-V.

[42] H.J. Berendsen, D. van der Spoel, R. van Drunen, GROMACS: a message-passing parallel molecular dynamics implementation, Comput. Phys. Commun. 91 (1–3) (1995) 43–56, https://doi.org/10.1016/0010-4655(95)00042-E.

[43] C. Oostenbrink, et al., A biomolecular force field based on the free enthalpy of hydration and solvation: the GROMOS force-field parameter sets 53A5 and 53A6, J. Comput. Chem. 25 (13) (2004) 1656–1676, https://doi.org/10.1002/jcc.20090.

[44] S. Dallakyan, A.J. Olson, Small-molecule Library Screening by Docking with PyRx, in Chemical Biology, Springer, 2015, pp. 243–250.

[45] M. Frisch, et al., EM64L-Gaussian 09, Revision D. 01, *Gaussian.* Inc., Wallingford CT, 2013.

[46] O. Trott, A.J. Olson, AutoDock Vina, Improving the speed and accuracy of docking with a new scoring function, efficient optimization, and multithreading, J. Comput. Chem. 31 (2) (2010) 455–461, https://doi.org/10.1002/jcc.21334.

[47] Y. Li, et al., Amyloid fibril structure of α-synuclein determined by cryo-electron microscopy, Cell Res. 28 (9) (2018) 897–903, https://doi.org/10.1038/s41422-018-0075-x.

[48] A.W. Schüttelkopf, D.M. Van Aalten, PRODRG: a tool for high-throughput crystallography of protein–ligand complexes, Acta Crystallogr. Sect. D Biol. Crystallogr. 60 (8) (2004) 1355–1363, https://doi.org/10.1107/S0907444904011679.

[49] J.A. Lemkul, W.J. Allen, D.R. Bevan, Practical considerations for building GROMOS-compatible small-molecule topologies, J. Chem. Inf. Model. 50 (12) (2010) 2221–2235, https://doi.org/10.1021/ci100335w.

[50] A. Pullman, Intermolecular Forces, vol. 14, Springer Science & Business Media, 2013.

[51] A. Lemak, N. Balabaev, On the Berendsen thermostat, Mol. Simulat. 13 (3) (1994) 177–187, https://doi.org/10.1080/08927029408021981.

[52] M. Parrinello, A. Rahman, Polymorphic transitions in single crystals: a new molecular dynamics method, J. Appl. Phys. 52 (12) (1981) 7182–7190, https://doi.org/10.1063/1.328693.

[53] A. Rahman, F.H. Stillinger, Molecular dynamics study of liquid water, J. Chem. Phys. 55 (7) (1971) 3336–3359, https://doi.org/10.1063/1.1676585.

[54] T. Darden, D. York, L. Pedersen, Particle mesh Ewald: an N· log (N) method for Ewald sums in large systems, J. Chem. Phys. 98 (12) (1993) 10089–10092, https://doi.org/10.1063/1.464397.

[55] U. Essmann, et al., A smooth particle mesh Ewald method, J. Chem. Phys. 103 (19) (1995) 8577–8593, https://doi.org/10.1063/1.470117.

[56] Z. Liu, Y. Huang, Advantages of proteins being disordered, Protein Sci. 23 (5) (2014) 539–550, https://doi.org/10.1002/pro.2443.

[57] V.K. Meena, V. Kumar, S. Karalia, J. Mol. Liq. 336 (2021), 116176, https://doi.org/10.1016/j.molliq.2021.116176.

[58] R.L. Jayaraj, N. Elangovan, In silico identification of potent inhibitors of alpha-synuclein aggregation and its in vivo evaluation using MPTP induced Parkinson mice model, Biomed. Aging Pathol. 4 (2) (2014) 147–152.